

1 Supporting Information:

2 Depletion of atmospheric gaseous elemental mercury by plant
3 uptake at Mt. Changbai, Northeast China

4 Xuewu Fu¹, Wei Zhu¹, Hui Zhang¹, Jonas Sommar¹, Xu Yang¹, Xun Wang^{1,2}, Che-Jen Lin^{1,3,4}, Xinbin Feng^{1,*}

5 ¹State Key Laboratory of Environmental Geochemistry, Institute of Geochemistry, Chinese Academy of
6 Sciences, 99 Lincheng West Road, Guiyang, 550081, China

7 ²University of the Chinese Academy of Sciences, Beijing 100049, China

8 ³Department of Civil and Environmental Engineering, Lamar University, Beaumont, Texas 77710, United States

9 ⁴Center for Advances in Water and Air Quality, Lamar University, Beaumont, Texas 77710, United States

10
11 Correspondence to: Xinbin Feng (fengxinbin@vip.skleg.cn)

13 1 Supplementary Text.....	Page S1
14 1.1 Nocturnal boundary layer.....	Page S1
15 1.2 Simulations of atmospheric GEM at Mt. Changbai forest using a box model.....	Page S1
16 1.3 The turbulent diffusivity (Kc).....	Page S2
17 Figure S1.....	Page S3
18 Figure S2.....	Page S4
19 Figure S3.....	Page S5
20 Figure S4.....	Page S6
21 Figure S5.....	Page S7
22 Figure S6.....	Page S8
23 Figure S7.....	Page S9
24 Table S1	Page S10
25 Table S2	Page S11
26 Table S3	Page S12
27 Table S4	Page S13
28 Table S5	Page S14
29 Reference.....	Page S15-S17

30 **1 Supplementary Text**

31 **1.1 Nocturnal boundary layer**

32 The Nocturnal boundary layer (NBL) was calculated by Weather Research and
33 Forecasting Model (WRF) 3.5 with two-way nested runs. The spatial resolution for
34 course domain is 30 km with 100×100 grid cells, and for the nested domain is 10 km
35 with 30×30 grid cells. As our studied site is 100-200 km away from Sea of Japan, we
36 chose the MYJ scheme for NBL as earlier studies suggested that MYJ scheme was as
37 first choice for marine atmospheric boundary layer simulations without *a*
38 *priori* information of atmospheric stability in the region of interest (Huang et al.,
39 2013; Krogsæter and Reuder, 2015). For other parameterizations, we selected Kain
40 and Fritsch cumulus scheme for cumulus parameterization, Lin (Purdue) scheme for
41 microphysics options RRTM scheme for Radiation Physics Options.

42

43

44 **1.2 Simulations of atmospheric GEM at Mt. Changbai forest using a box model**

45 A box model was applied to estimate the GEM concentration at the height of 24
46 m agl. Based on the measured characteristics of the GEM depletion events, the
47 model assumes that vegetative uptake (in terms of dry deposition flux) is the only
48 pathway for the GEM removal and chemical transformation is not included in the box
49 modeling. A sensitivity analysis was performed on three parameters: (1) dry
50 deposition flux ($0\text{-}10 \text{ ng m}^{-2} \text{ h}^{-1}$, the range of measured deposition flux using flux
51 bags), (2) turbulent diffusivity of the atmosphere ($0.1\text{-}10 \text{ cm s}^{-1}$, typical value under
52 low wind condition), and (3) a typical nocturnal boundary layer height (100 m agl).
53 GEM concentration above the stable nocturnal boundary layer was assigned to 1.56 ng m^{-3} ,
54 the mean observed at 45 m during daytime when the vertical mixing is strong.
55 The flux of vegetative uptake (F_C) and the resulted concentration gradient was
56 calculated based on the on the algorithm:

$$F_C^{AGM} = - \underbrace{\frac{\kappa \cdot u_*}{\Phi_H(\zeta_1)}}_{K_C} \cdot \frac{\partial C}{\partial \ln(z)} \quad (1)$$

57 where κ is von Kármán constant (~ 0.41), u_* is the friction velocity (m s^{-1}), $\psi_H(\zeta_1)$ is
58 the integrated universal function for sensible heat to correct for deviations from the
59 ideal logarithmic profile, K_C term is the turbulent diffusivity (m s^{-1}), C is the
60 ideal logarithmic profile, K_C term is the turbulent diffusivity (m s^{-1}), C is the

61 concentration parameter for GEM concentration (ng m^{-3}), z is the height parameter
62 (m).

63

64 **1.3 The turbulent diffusivity (K_c)**

65 The flux-gradient approach (Kaimal and Finnigan, 1994) expresses a scalar flux (F , e.g.
66 $\text{ng m}^{-2} \text{s}^{-1}$) as the product between the turbulent diffusivity (K_C , $\text{m}^2 \text{s}^{-1}$) and a concentration
67 gradient ($\partial c / \partial z$, ng m^{-4}) assuming that measurements are made within a vertical layer of
68 constant flux that forms over homogeneous terrain:

69
$$F = -K_C \cdot \frac{\partial c}{\partial z} = -\frac{u_* \cdot \kappa \cdot (z-d)}{\phi_H(\varsigma)} \cdot \frac{\partial c}{\partial z} = -\frac{u_* \cdot \kappa}{\phi_H(\varsigma)} \cdot \frac{\partial c}{\partial \ln z} \quad (2),$$

70 where, u_* is the friction velocity (m s^{-1}), κ is the von Kármán constant (taken as 0.4),
71 $\phi_H(\varsigma)$ is the diabatic influence function for heat (parameterized as a function of
72 $\varsigma = (z-d)/L$, where L is the Obukhov length), whereas z and d are the
73 measurement and (canopy) displacement height (m) respectively. An empirical form of
74 $\phi_H(\varsigma)$ is $0.95/\sqrt{(1-11.6\varsigma)}$ and $0.95 + 7.8\varsigma$ for unstable ($\varsigma < 0$) and stable ($2 > \varsigma \geq 0$)
75 atmospheric conditions respectively (Foken, 2008).

76

77 For flux-gradient measurements made within the roughness sublayer above the canopy
78 height (i.e. $h_{\text{canopy}} < z < z_*$), Eq. 1 is not valid (*underestimates* the magnitude of scalar
79 flux) and requires further correction following e.g. Garratt (Garratt, 1992) and Simpson et al.
80 (Simpson et al., 1998):

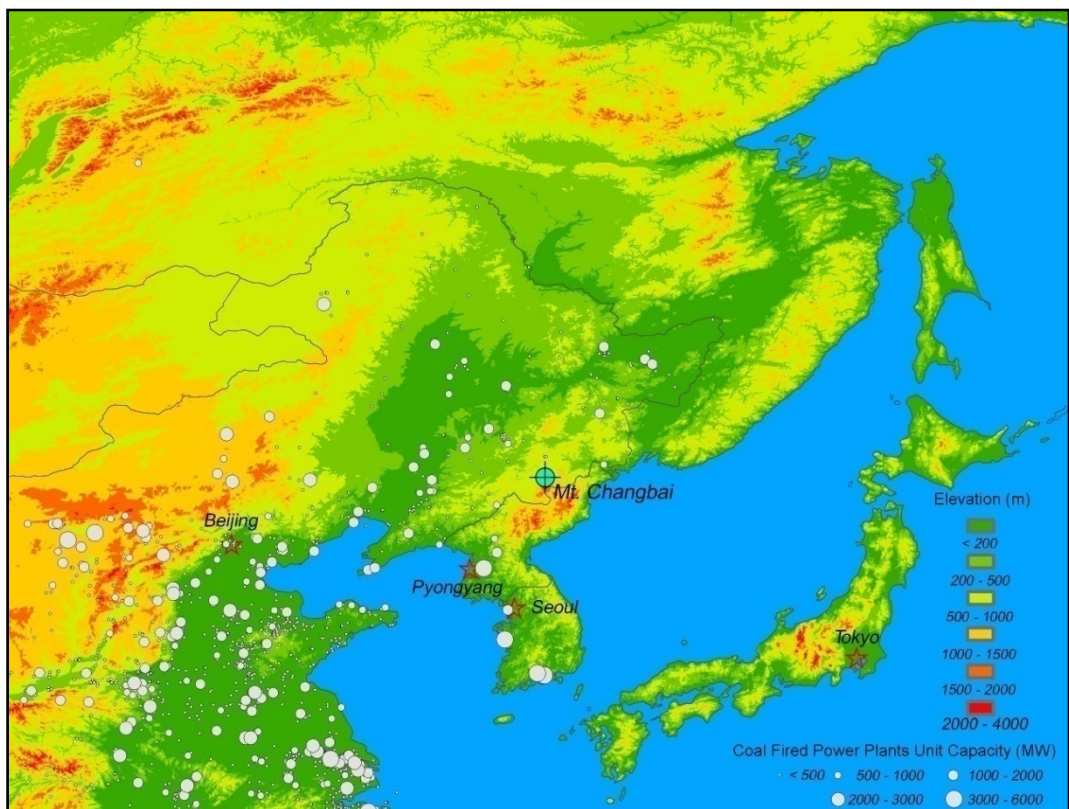
81
$$F = -\frac{u_* \cdot \kappa \cdot (z-d)}{\phi_h(\varsigma) \cdot \phi_*(z/z_*)} \cdot \frac{\partial c}{\partial z} \quad (3)$$

82 In contrast to $\phi_H(\varsigma)$, the additional correction function $\phi_*(z/z_*)$ in Eq. 2 is independent of
83 stability. A common type of parameterization for ϕ_* is $\exp[-0.7(1 - \frac{z}{z_*})]$ (Garratt, 1992).

84 In-turn, the upper limit of the roughness sublayer (z_*) can be estimated by $2 \cdot h_{\text{canopy}} - d$
85 (Raupach, 1994).

86

87 | Figure S1. Map showing the location of Mt. Changbai forest and coal fired power plants in
88 Northeast Asia.



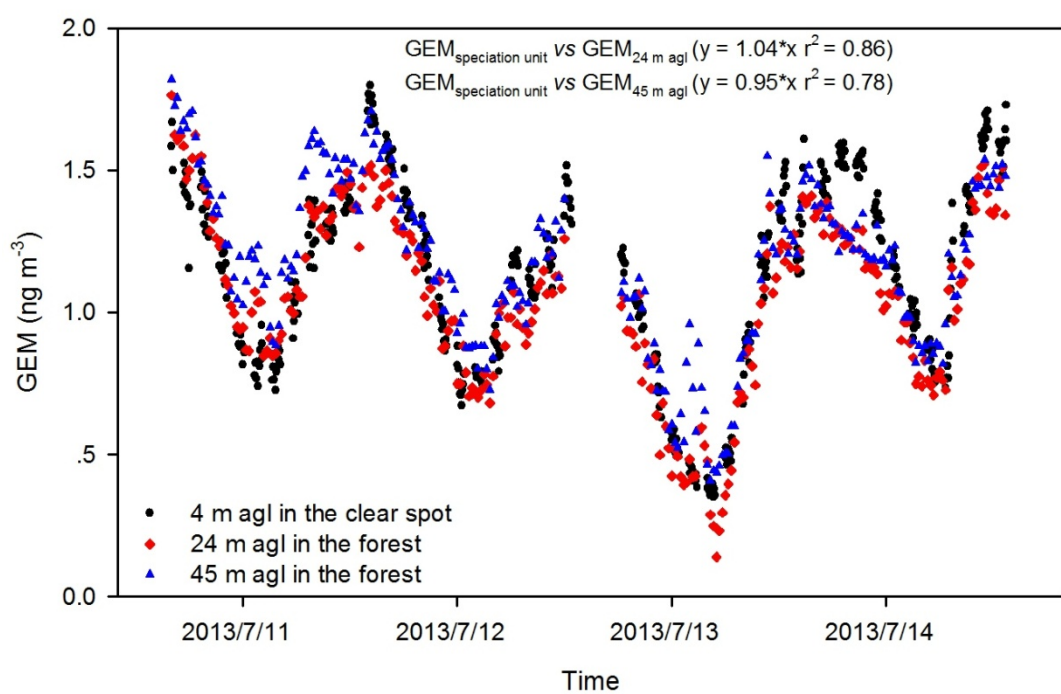
89

90

91

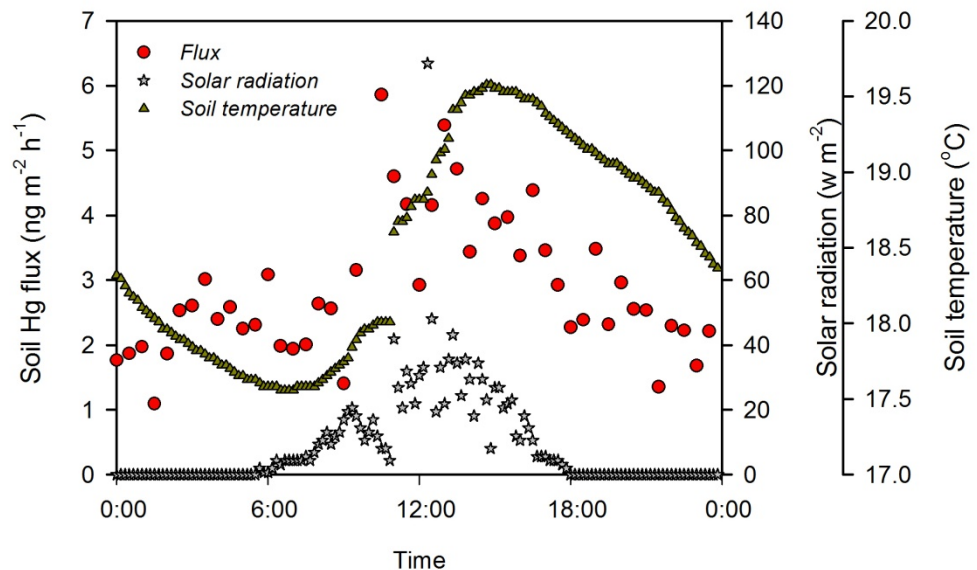
92

93 | Figure S2. GEM at 4 m agl in the clear spot measured by the Tekran speciation unit, 24 m agl (~3
94 | m above forest canopy, long-term GEM sampling site) and 45 m agl (~24 m above forest
95 | canopy) measured by the Tekran 2537 from 10 to 14 July 2013.



96
97
98
99

100 | Figure S3. Time series of soil/air GEM flux and meteorological parameters in Mt. Changbai forest
101 in July 2013.



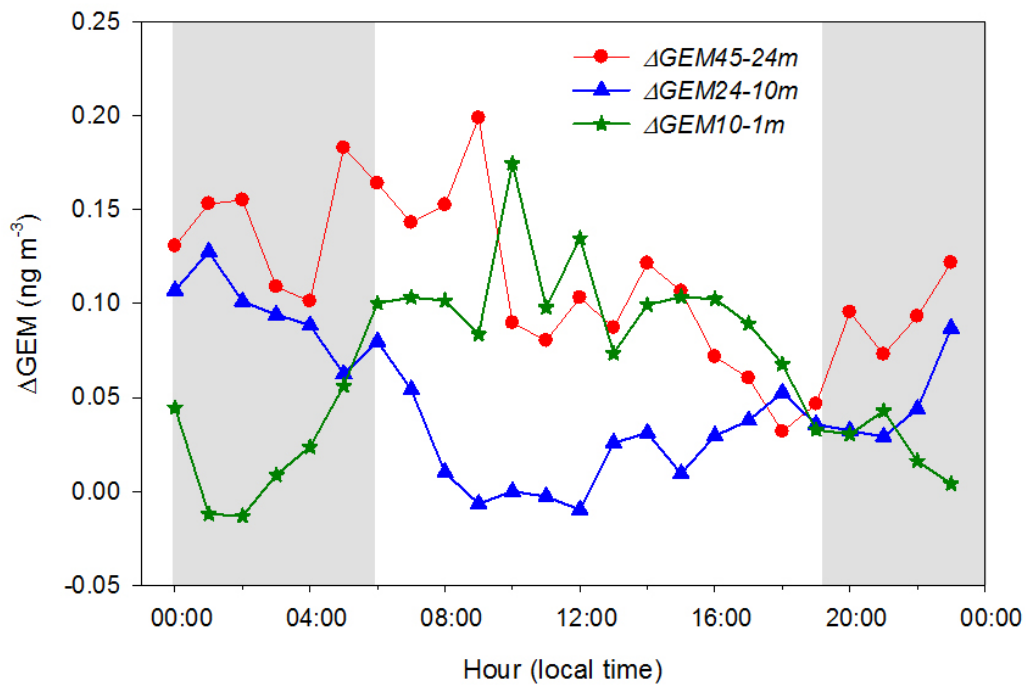
102

103

104

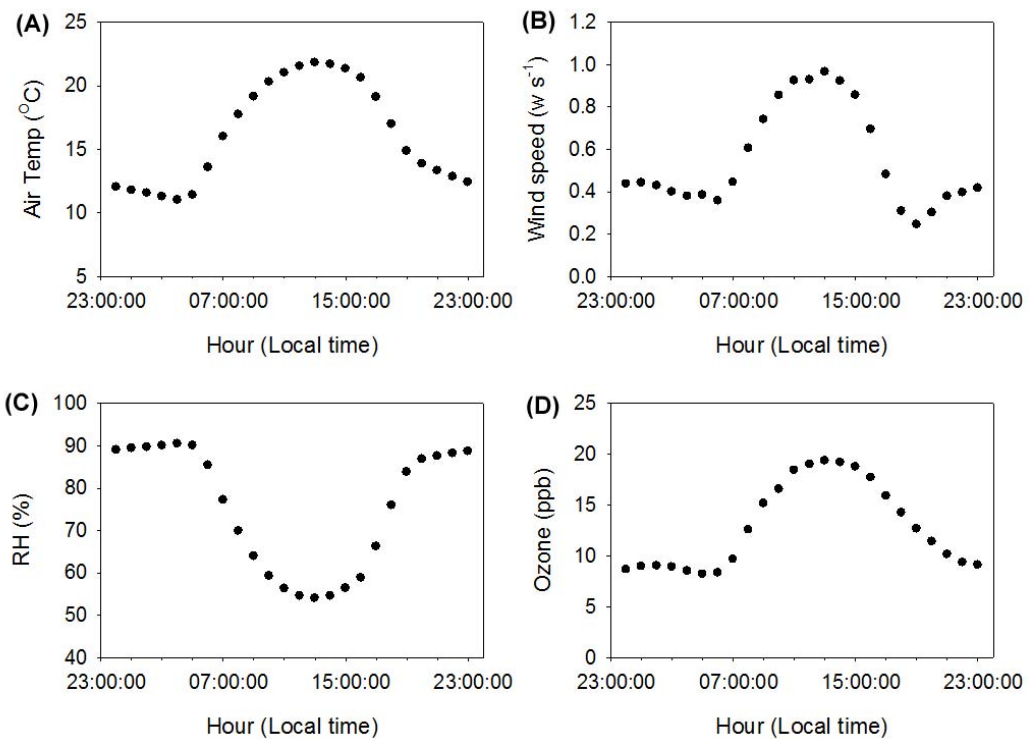
105

106 | Figure S4. Diurnal trends in vertical gradient of GEM concentrations between the height of 45-24
107 m, 24-10 m and 10-1m in Mt. Changbai forest from 10 to 15 July 2013.



108
109
110
111

112 | Figure S5. Diurnal variations of air temperature (A), wind speed (B), relative humidity (RH, C)
113 and ozone concentrations (D) in Mt. Changbai forest in leaf-growing season from October 2008 to
114 December 2014.



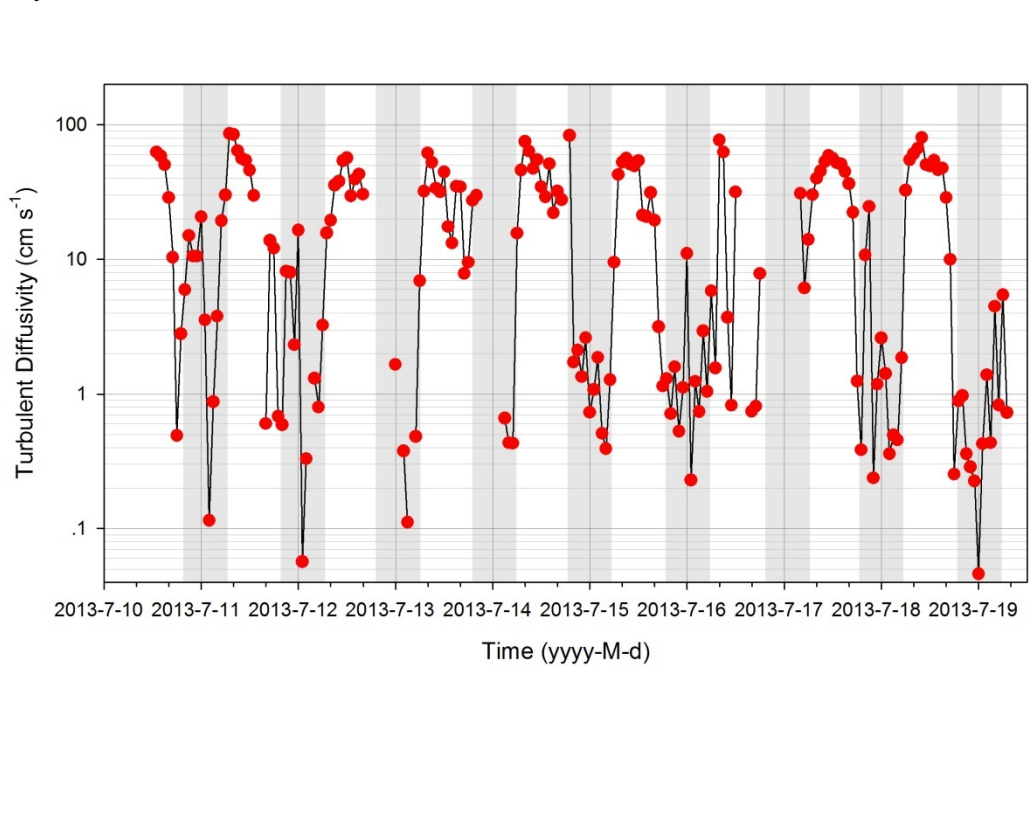
115

116

117

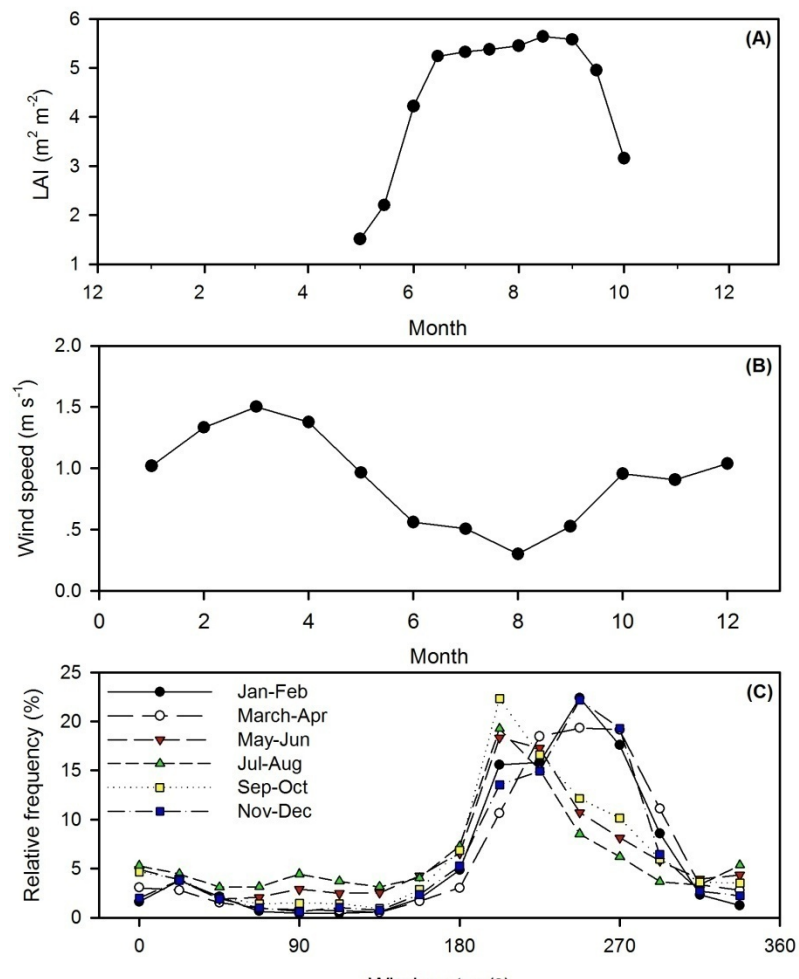
118

119 | Figure S6. Temporal variation of the turbulent diffusivity at Mt. Changbai forest from 10 to 19
120 July 2013



121
122
123
124

125 | Figure S7. Wind frequency distributions in leaf-growing season and non-leaf-growing season from
126 | Aug 2009 to Jul 2013 (A), monthly mean wind speed from Aug 2009 to Jul 2013 (B), and Leaf
127 | areas index in leaf-growing season during 2003-2005(C) (Shi et al., 2008).



128

129

130 Table S1. Statistical summary of litterfall Hg concentrations and litter mass in Mt. Changbai forest

Litterfall collection site	Time	Species	Concentration (ng g ⁻¹)	Litter mass (g m ⁻²)	Mass-weight concentration (ng g ⁻¹)
Collector-1	2013-09	<i>Pinus koraiensis</i>	44.5	51.70	
		<i>Acer pseudo-sieboldianum</i>	138.5	24.95	
		<i>Quercus mongolica</i>	170.4	35.60	74.8
		<i>Fraxinus mandshurica</i>	44.5	51.70	
		<i>Tilia amurensis</i>	138.5	24.95	
Collector-1	2013-10	<i>Others</i>	170.4	35.60	
		<i>Acer mono</i>	60.2	1.8	60.2
Collector-2	2013-09	<i>Pinus koraiensis</i>	40.4	6.48	
		<i>Acer pseudo-sieboldianum</i>	46.8	5.38	
		<i>Quercus mongolica</i>	31.2	9.49	
		<i>Acer mono</i>	58.0	4.81	39.7
		<i>Fraxinus mandshurica</i>	34.5	18.54	
Collector-2	2013-10	<i>Tilia amurensis</i>	45.7	52.12	
		<i>Others</i>	36.80	91.16	
		<i>Pinus koraiensis</i>	34.1	4.4	
		<i>Quercus mongolica</i>	30.3	8.8	53.3
Collector-3	2013-09	<i>Acer mono</i>	70.7	5.8	
		<i>Others</i>	81.3	6.6	
		<i>Acer ginnala Maxim</i>	38.1	5.8	
		<i>Pinus koraiensis</i>	29.4	19.0	
		<i>Acer pseudo-sieboldianum</i>	49.6	4.6	
Collector-3	2013-10	<i>Quercus mongolica</i>	32.5	10.8	
		<i>Acer mono</i>	46.9	6.0	31.1
		<i>Fraxinus mandshurica</i>	23.4	1.5	
		<i>Tilia amurensis</i>	40.4	19.6	
		<i>Others</i>	29.8	283.3	
Collector-4	2013-09	<i>Pinus koraiensis</i>	21.7	1.5	
		<i>Quercus mongolica</i>	42.3	3.2	35.8
		<i>Others</i>	31.4	70.6	
Collector-4	2013-10	<i>Acer pseudo-sieboldianum</i>	47.4	2.7	
		<i>Quercus mongolica</i>	26.3	4.1	
		<i>Acer mono</i>	50.9	15.5	34.2
		<i>Tilia amurensis</i>	43.0	11.8	
		<i>Others</i>	32.8	121.1	
Collector-4	2013-10	<i>Pinus koraiensis</i>	40.1	19.4	
		<i>Quercus mongolica</i>	46.0	21.7	64.4
		<i>Others</i>	100.9	23.9	
Overall mean				43.0±29.5	

132 Table S2. Concentration of atmospheric speciated Hg (GEM, PBM, and GOM) and isotopic
 133 composition of atmospheric GEM at Mt. Changbai forest

Sample ID	Sampling period	GEM conc.	PBM conc.	GOM conc.	$\delta^{202}\text{Hg}$	$\delta^{202}\text{Hg}$	$\Delta^{199}\text{Hg}$	$\Delta^{199}\text{Hg}$	$\Delta^{200}\text{Hg}$	$\Delta^{200}\text{Hg}$	$\Delta^{201}\text{Hg}$	$\Delta^{201}\text{Hg}$
		ng m ⁻³	pg m ⁻³	pg m ⁻³	%o	2σ, %o						
GEM-1	2013/7/8 13:40-2013/7/9 15:30	1.60	2	4	-0.06	0.09	-0.05	0.04	0.01	0.04	-0.01	0.06
GEM-2	2013/7/9 15:30-2013/7/10 15:30	1.46	2	2	0.35	0.09	-0.05	0.04	-0.04	0.04	-0.12	0.06
GEM-3	2013/7/10 15:30-2013/7/11 15:45	1.23	4	2	0.61	0.09	-0.09	0.04	-0.05	0.04	-0.08	0.06
GEM-4	2013/7/11 15:45-2013/7/12 15:50	1.14	5	2	0.80	0.09	-0.08	0.04	-0.03	0.04	-0.06	0.06
GEM-5	2013/7/12 15:50-2013/7/13 16:00	0.91	6	1	0.91	0.09	-0.06	0.04	-0.04	0.04	-0.07	0.06
GEM-6	2013/7/13 16:00-2013/7/14 15:40	1.32	4	2	0.58	0.09	-0.06	0.04	-0.06	0.04	-0.05	0.06
GEM-7	2013/7/14 15:40-2013/7/15 17:10	1.37	2	2	0.58	0.09	-0.08	0.04	-0.05	0.04	-0.04	0.06
GEM-8	2013/7/15 17:15-2013/7/16 17:30	1.24	2	2	0.08	0.09	-0.04	0.04	-0.04	0.04	-0.04	0.06
GEM-9	2013/7/16 17:30-2013/7/17 18:10	1.57	5	1	-0.34	0.09	-0.11	0.04	-0.04	0.04	-0.06	0.06
GEM-10	2013/7/17 18:10-2013/7/18 18:35	1.30	8	1	-0.01	0.09	-0.08	0.04	-0.05	0.04	-0.04	0.06

134

135

136 Table S3. A statistical summary of reported litterfall Hg deposition fluxes and estimated annual
 137 litterfall Hg deposition of Hg over the world.

Region	Litterfall Hg deposition flux ($\mu\text{g m}^{-2} \text{yr}^{-1}$)			Forest area (km^2)	Estimated litterfall deposition (Mg yr^{-1})	Reference
	Range	Median	N			
Asia	20.9-220	37.5±76.1	6	5,775,220	217	(Wang et al., 2009;Fu et al., 2010a;Fu et al., 2010b;Zhou et al., 2013)
North America	3.8-30.9	13.9±5.6	47	6,847,010	95	(Lindberg, 1996;Rea et al., 1996;Grigal et al., 2000;St Louis et al., 2001;Sheehan et al., 2006;Demers et al., 2007;Bushey et al., 2008;Fisher and Wolfe, 2012;Juillerat et al., 2012;Risch et al., 2012;Benoit et al., 2013)
Europe (including Russia)	2.7-25.2	14.2±8.9	6	10,156,300	144	(Iverfeldt, 1991;Munthe et al., 1995;Lee et al., 2000;Schwesig and Matzner, 2000;Lindberg et al., 2007;Larssen et al., 2008)
South America	43.0-184	60.0±49.0	9	9,436,410	566	(Roulet et al., 1998;Fostier et al., 2003;Mélières et al., 2003;Silva-Filho et al., 2006;Teixeira et al., 2012)
Africa				6,164,310	159*	Lack of observational data
Oceania				1,951,370	50*	Lack of observational data
Global total					1232	

138 (Estimated litterfall deposition: * indicates the values were calculated using the global median litterfall Hg deposition flux and the forest
 139 area in these regions)

140
 141

142 Table S4. A statistical summary of reported throughfall Hg deposition fluxes and estimated annual
 143 throughfall Hg deposition of Hg over the world

Region	Throughfall Hg deposition flux			Forest area (km ²)	Estimated throughfall deposition (mg yr ⁻¹)	Reference			
	(µg m ⁻² yr ⁻¹)								
	Range	Median	N						
Asia	10.5-71.3	36.8±29.9	4	5,775,220	213	(Wan et al., 2009; Wang et al., 2009; Fu et al., 2010a; Fu et al., 2010b)			
North America	3.8-30.9	11.8±3.3	10	6,847,010	81	(Lindberg, 1996; Rea et al., 1996; Grigal et al., 2000; St Louis et al., 2001; Sheehan et al., 2006; Choi et al., 2008; Fisher and Wolfe, 2012)			
Europe (including Russia)	6.8-39.0	15.2±10.7	8	10,156,300	154	(Iverfeldt, 1991; Munthe et al., 1995; Lee et al., 2000; Schwesig and Matzner, 2000; Lindberg et al., 2007; Larssen et al., 2008)			
South America	72	72	1	9,436,410	679	(Fostier et al., 2000)			
Africa				6,164,310	160*	Lack of observational data			
Oceania				1,951,370	51*	Lack of observational data			
Global total					1338				

144 (Estimated throughfall deposition: * indicates the values were calculated using the global median throughfall Hg deposition flux and the
 145 forest area in these regions)

146

147

148

149 Table S5. A statistical summary of reported forest soil emission fluxes and estimated annual forest
 150 soil emission fluxes over the world
 151

Region	Forest soil Hg emission flux			Forest area (km ²)	Estimated forest soil emission (Mg yr ⁻¹)	Reference
	Range	Median	N			
Asia	3.3-81.2	30.4±23.5	11	5,775,220	176	(Wang et al., 2006;Fu et al., 2008;Fu et al., 2012;Ma et al., 2013)
North America	-1.3-45.9	9.2±11.4	15	6,847,010	63	(Carpi and Lindberg, 1998;Poissant and Casimir, 1998;Zhang et al., 2001;Nacht and Gustin, 2004;Schroeder et al., 2005;Kuiken et al., 2008a;Kuiken et al., 2008b;Choi and Holsen, 2009)
Europe (including Russia)	-0.1-9.6	2.4±4.3	4	10,156,300	24	(Schroeder et al., 1989;Xiao et al., 1991;Ferrara et al., 1997;Lindberg et al., 1998)
South America	6.0	6.0	1	9,436,410	57	(Carpi et al., 2014)
Africa				6,164,310	47*	Lack of observational data
Oceania				1,951,370	15*	Lack of observational data
Global total					381	

152 (Estimated forest soil emission: * indicates the values were calculated using the global median forest soil Hg emission flux and the forest
 153 area in these regions)

154
 155
 156

157 **Reference:**

- 158 Benoit, J. M., Cato, D. A., Denison, K. C., and Moreira, A. E.: Seasonal Mercury Dynamics in a New
159 England Vernal Pool, *Wetlands*, 33, 887-894, DOI 10.1007/s13157-013-0447-4, 2013.
- 160 Bushey, J. T., Nallana, A. G., Montesdeoca, M. R., and Driscoll, C. T.: Mercury dynamics of a northern
161 hardwood canopy, *Atmos Environ*, 42, 6905-6914, DOI 10.1016/j.atmosenv.2008.05.043, 2008.
- 162 Carpi, A., and Lindberg, S. E.: Application of a Teflon (TM) dynamic flux chamber for quantifying soil
163 mercury flux: Tests and results over background soil, *Atmos Environ*, 32, 873-882, Doi
164 10.1016/S1352-2310(97)00133-7, 1998.
- 165 Carpi, A., Fostier, A. H., Orta, O. R., dos Santos, J. C., and Gittings, M.: Gaseous mercury emissions
166 from soil following forest loss and land use changes: Field experiments in the United States and Brazil,
167 *Atmos Environ*, 96, 423-429, DOI 10.1016/j.atmosenv.2014.08.004, 2014.
- 168 Choi, H. D., Sharac, T. J., and Holsen, T. M.: Mercury deposition in the Adirondacks: A comparison
169 between precipitation and throughfall, *Atmos Environ*, 42, 1818-1827, DOI
170 10.1016/j.atmosenv.2007.11.036, 2008.
- 171 Choi, H. D., and Holsen, T. M.: Gaseous mercury fluxes from the forest floor of the Adirondacks,
172 *Environ Pollut*, 157, 592-600, DOI 10.1016/j.envpol.2008.08.020, 2009.
- 173 Demers, J. D., Driscoll, C. T., Fahey, T. J., and Yavitt, J. B.: Mercury cycling in litter and soil in
174 different forest types in the Adirondack region, New York, USA, *Ecol Appl*, 17, 1341-1351, Doi
175 10.1890/06-1697.1, 2007.
- 176 Ferrara, R., Maserti, B. E., Andersson, M., Edner, H., Ragnarson, P., and Svanberg, S.: Mercury
177 degassing rate from mineralized areas in the Mediterranean basin, *Water Air Soil Poll*, 93, 59-66, Doi
178 10.1023/A:1022107205659, 1997.
- 179 Fisher, L. S., and Wolfe, M. H.: Examination of mercury inputs by throughfall and litterfall in the Great
180 Smoky Mountains National Park, *Atmos Environ*, 47, 554-559, DOI 10.1016/j.atmosenv.2011.10.017,
181 2012.
- 182 Foken, T.: *Micrometeorology*, Springer-Verlag, Berlin, Heidelberg, 2008.
- 183 Fostier, A. H., Forti, M. C., Guimaraes, J. R. D., Melfi, A. J., Boulet, R., Santo, C. M. E., and Krug, F.
184 J.: Mercury fluxes in a natural forested Amazonian catchment (Serra do Navio, Amapa State, Brazil),
185 *Sci Total Environ*, 260, 201-211, Doi 10.1016/S0048-9697(00)00564-7, 2000.
- 186 Fostier, A. H., Cecon, K., and Forti, M. C.: Urban influence on litterfall trace metals fluxes in the
187 Atlantic forest of Sao Paulo (Brazil), *J Phys Iv*, 107, 491-494, Doi 10.1051/Jp4:20030348, 2003.
- 188 Fu, X., Feng, X., Zhu, W., Rothenberg, S., Yao, H., and Zhang, H.: Elevated atmospheric deposition
189 and dynamics of mercury in a remote upland forest of southwestern China, *Environ Pollut*, 158,
190 2324-2333, 10.1016/j.envpol.2010.01.032, 2010a.
- 191 Fu, X. W., Feng, X. B., and Wang, S. F.: Exchange fluxes of Hg between surfaces and atmosphere in
192 the eastern flank of Mount Gongga, Sichuan province, southwestern China, *J Geophys Res-Atmos*, 113,
193 Artn D20306
194 Doi 10.1029/2008jd009814, 2008.
- 195 Fu, X. W., Feng, X., Dong, Z. Q., Yin, R. S., Wang, J. X., Yang, Z. R., and Zhang, H.: Atmospheric
196 gaseous elemental mercury (GEM) concentrations and mercury depositions at a high-altitude mountain
197 peak in south China, *Atmos Chem Phys*, 10, 2425-2437, 2010b.
- 198 Fu, X. W., Feng, X. B., Zhang, H., Yu, B., and Chen, L. G.: Mercury emissions from natural surfaces
199 highly impacted by human activities in Guangzhou province, South China, *Atmos Environ*, 54,
200 185-193, DOI 10.1016/j.atmosenv.2012.02.008, 2012.

- 201 Garratt, J. R.: The atmospheric boundary layer, Cambridge University Press, Cambridge, UK, 1992.
- 202 Grigal, D. F., Kolkka, R. K., Fleck, J. A., and Nater, E. A.: Mercury budget of an upland-peatland
203 watershed, *Biogeochemistry*, 50, 95-109, Doi 10.1023/A:1006322705566, 2000.
- 204 Huang, H. Y., Hall, A., and Teixeira, J.: Evaluation of the WRF PBL Parameterizations for Marine
205 Boundary Layer Clouds: Cumulus and Stratocumulus, *Mon Weather Rev*, 141, 2265-2271,
206 10.1175/Mwr-D-12-00292.1, 2013.
- 207 Iverfeldt, A.: Mercury in forest canopy throughfall water and its relation to atmospheric deposition,
208 *Water Air Soil Poll*, 56, 553-564, Doi 10.1007/Bf00342299, 1991.
- 209 Juillerat, J. I., Ross, D. S., and Bank, M. S.: Mercury in litterfall and upper soil horizons in forested
210 ecosystems in Vermont, USA, *Environ Toxicol Chem*, 31, 1720-1729, Doi 10.1002/etc.1896, 2012.
- 211 Kaimal, J. C., and Finnigan, J. J.: Atmospheric Boundary Layer Flows, Oxford University Press, New
212 York, Oxford, 1994.
- 213 Krogsaeter, O., and Reuder, J.: Validation of boundary layer parameterization schemes in the Weather
214 Research and Forecasting (WRF) model under the aspect of offshore wind energy applicationspart II:
215 boundary layer height and atmospheric stability, *Wind Energy*, 18, 1291-1302, 10.1002/we.1765, 2015.
- 216 Kuiken, T., Gustin, M., Zhang, H., Lindberg, S., and Sedinger, B.: Mercury emission from terrestrial
217 background surfaces in the eastern USA. II: Air/surface exchange of mercury within forests from South
218 Carolina to New England, *Appl Geochem*, 23, 356-368, DOI 10.1016/j.apgeochem.2007.12.007,
219 2008a.
- 220 Kuiken, T., Zhang, H., Gustin, M., and Lindberg, S.: Mercury emission from terrestrial background
221 surfaces in the eastern USA. Part I: Air/surface exchange of mercury within a southeastern deciduous
222 forest (Tennessee) over one year, *Appl Geochem*, 23, 345-355, DOI 10.1016/j.apgeochem.2007.12.006,
223 2008b.
- 224 Larssen, T., de Wit, H. A., Wiker, M., and Halse, K.: Mercury budget of a small forested boreal
225 catchment in southeast Norway, *Sci Total Environ*, 404, 290-296, DOI 10.1016/j.scitotenv.2008.03.013,
226 2008.
- 227 Lee, Y. H., Bishop, K. H., and Munthe, J.: Do concepts about catchment cycling of methylmercury and
228 mercury in boreal catchments stand the test of time? Six years of atmospheric inputs and runoff export
229 at Svatberget, northern Sweden, *Sci Total Environ*, 260, 11-20, Doi 10.1016/S0048-9697(00)00538-6,
230 2000.
- 231 Lindberg, S., Bullock, R., Ebinghaus, R., Engstrom, D., Feng, X. B., Fitzgerald, W., Pirrone, N.,
232 Prestbo, E., and Seigneur, C.: A synthesis of progress and uncertainties in attributing the sources of
233 mercury in deposition, *Ambio*, 36, 19-32, 2007.
- 234 Lindberg, S. E.: Forests and the global biogeochemical cycle of mercury: The importance of
235 understanding air/vegetation exchange processes, *Nato Asi* 2, 21, 359-380, 1996.
- 236 Lindberg, S. E., Hanson, P. J., Meyers, T. P., and Kim, K. H.: Air/surface exchange of mercury vapor
237 over forests - The need for a reassessment of continental biogenic emissions, *Atmos Environ*, 32,
238 895-908, Doi 10.1016/S1352-2310(97)00173-8, 1998.
- 239 Mélières, M. A., Pourchet, M., Charles-Dominique, P., and Gaucher, P.: Mercury in canopy leaves of
240 French Guiana in remote areas, *Sci Total Environ*, 311, 261-267, Doi 10.1016/S0048-9697(03)00142-6,
241 2003.
- 242 Ma, M., Wang, D. Y., Sun, R. G., Shen, Y. Y., and Huang, L. X.: Gaseous mercury emissions from
243 subtropical forested and open field soils in a national nature reserve, southwest China, *Atmos Environ*,
244 64, 116-123, DOI 10.1016/j.atmosenv.2012.09.038, 2013.

- 245 Munthe, J., Hultberg, H., and Iverfeldt, A.: Mechanisms of Deposition of Methylmercury and Mercury
246 to Coniferous Forests, Water Air Soil Poll, 80, 363-371, Doi 10.1007/Bf01189686, 1995.
- 247 Nacht, D. M., and Gustin, M. S.: Mercury emissions from background and altered geologic units
248 throughout Nevada, Water Air Soil Poll, 151, 179-193, Doi 10.1023/B:Wate.0000009907.49577.A8,
249 2004.
- 250 Poissant, L., and Casimir, A.: Water-air and soil-air exchange rate of total gaseous mercury measured at
251 background sites, Atmos Environ, 32, 883-893, Doi 10.1016/S1352-2310(97)00132-5, 1998.
- 252 Raupach, M. R.: Simplified Expressions for Vegetation Roughness Length and Zero-Plane
253 Displacement as Functions of Canopy Height and Area Index, Bound-Lay Meteorol, 71, 211-216, Doi
254 10.1007/Bf00709229, 1994.
- 255 Rea, A. W., Keeler, G. J., and Scherbatskoy, T.: The deposition of mercury in throughfall and litterfall
256 in the lake Champlain watershed: A short-term study, Atmos Environ, 30, 3257-3263, Doi
257 10.1016/1352-2310(96)00087-8, 1996.
- 258 Risch, M. R., DeWild, J. F., Krabbenhoft, D. P., Kolka, R. K., and Zhang, L. M.: Litterfall mercury dry
259 deposition in the eastern USA, Environ Pollut, 161, 284-290, DOI 10.1016/j.envpol.2011.06.005, 2012.
- 260 Roulet, M., Lucotte, M., Saint-Aubin, A., Tran, S., Rheault, I., Farella, N., Da Silva, E. D., Dezencourt,
261 J., Passos, C. J. S., Soares, G. S., Guimaraes, J. R. D., Mergler, D., and Amorim, M.: The geochemistry
262 of mercury in central Amazonian soils developed on the Alter-do-Chao formation of the lower Tapajos
263 River Valley, Para state, Brazil, Sci Total Environ, 223, 1-24, Doi 10.1016/S0048-9697(98)00265-4,
264 1998.
- 265 Schroeder, W. H., Munthe, J., and Lindqvist, O.: Cycling of Mercury between Water, Air, and Soil
266 Compartments of the Environment, Water Air Soil Poll, 48, 337-347, 1989.
- 267 Schroeder, W. H., Beauchamp, S., Edwards, G., Poissant, L., Rasmussen, P., Tordon, R., Dias, G.,
268 Kemp, J., Van Heyst, B., and Banic, C. M.: Gaseous mercury emissions from natural sources in
269 Canadian landscapes, J Geophys Res-Atmos, 110, Artn D18302
270 Doi 10.1029/2004jd005699, 2005.
- 271 Schwesig, D., and Matzner, E.: Pools and fluxes of mercury and methylmercury in two forested
272 catchments in Germany, Sci Total Environ, 260, 213-223, Doi 10.1016/S0048-9697(00)00565-9, 2000.
- 273 Sheehan, K. D., Fernandez, I. J., Kahl, J. S., and Amirbahman, A.: Litterfall mercury in two forested
274 watersheds at Acadia National Park, Maine, USA, Water Air Soil Poll, 170, 249-265, DOI
275 10.1007/s11270-006-3034-y, 2006.
- 276 Shi, T. T., Guan, D. X., Wang, A. Z., Wu, J. B., Jin, C. J., and Han, S. J.: Comparison of three models to
277 estimate evapotranspiration for a temperate mixed forest, Hydrol Process, 22, 3431-3443,
278 10.1002/hyp.6922, 2008.
- 279 Silva-Filho, E. V., Machado, W., Oliveira, R. R., Sella, S. M., and Lacerda, L. D.: Mercury deposition
280 through litterfall in an Atlantic Forest at Ilha Grande, southeast Brazil, Chemosphere, 65, 2477-2484,
281 DOI 10.1016/j.chemosphere.2006.04.053, 2006.
- 282 Simpson, I. J., Thurtell, G. W., Neumann, H. H., Den Hartog, G., and Edwards, G. C.: The validity of
283 similarity theory in the roughness sublayer above forests, Bound-Lay Meteorol, 87, 69-99, Doi
284 10.1023/A:1000809902980, 1998.
- 285 St Louis, V. L., Rudd, J. W. M., Kelly, C. A., Hall, B. D., Rolphus, K. R., Scott, K. J., Lindberg, S. E.,
286 and Dong, W.: Importance of the forest canopy to fluxes of methyl mercury and total mercury to boreal
287 ecosystems, Environmental Science & Technology, 35, 3089-3098, Doi 10.1021/Es001924p, 2001.
- 288 Teixeira, D. C., Montezuma, R. C., Oliveira, R. R., and Silva, E. V.: Litterfall mercury deposition in

- 289 Atlantic forest ecosystem from SE - Brazil, Environ Pollut, 164, 11-15, DOI
290 10.1016/j.envpol.2011.10.032, 2012.
- 291 Wan, Q., Feng, X. B., Lu, J., Zheng, W., Song, X. J., Li, P., Han, S. J., and Xu, H.: Atmospheric
292 mercury in Changbai Mountain area, northeastern China II. The distribution of reactive gaseous
293 mercury and particulate mercury and mercury deposition fluxes, Environ Res, 109, 721-727, DOI
294 10.1016/j.envres.2009.05.006, 2009.
- 295 Wang, D. Y., He, L., Shi, X. J., Wei, S. Q., and Feng, X. B.: Release flux of mercury from different
296 environmental surfaces in Chongqing, China, Chemosphere, 64, 1845-1854, DOI
297 10.1016/j.chemosphere.2006.01.054, 2006.
- 298 Wang, Z. W., Zhang, X. S., Xiao, J. S., Zhijia, C., and Yu, P. Z.: Mercury fluxes and pools in three
299 subtropical forested catchments, southwest China, Environ Pollut, 157, 801-808, DOI
300 10.1016/j.envpol.2008.11.018, 2009.
- 301 Xiao, Z. F., Munthe, J., Schroeder, W. H., and Lindqvist, O.: Vertical Fluxes of Volatile Mercury over
302 Forest Soil and Lake Surfaces in Sweden, Tellus B, 43, 267-279, DOI
303 10.1034/j.1600-0889.1990.t01-1-00009.x-i1, 1991.
- 304 Zhang, H., Lindberg, S. E., Marsik, F. J., and Keeler, G. J.: Mercury air/surface exchange kinetics of
305 background soils of the Tahquamenon River watershed in the Michigan Upper Peninsula, Water Air
306 Soil Poll, 126, 151-169, Doi 10.1023/A:1005227802306, 2001.
- 307 Zhou, J., Feng, X. B., Liu, H. Y., Zhang, H., Fu, X. W., Bao, Z. D., Wang, X., and Zhang, Y. P.:
308 Examination of total mercury inputs by precipitation and litterfall in a remote upland forest of
309 Southwestern China, Atmos Environ, 81, 364-372, DOI 10.1016/j.atmosenv.2013.09.010, 2013.
- 310